# Involvement of high-mobility group box 1 in the pathogenesis of severe hemolytic uremic syndrome in a murine model

Ryo Maeda (1), Yukihiko Kawasaki (1-2)*, Yohei Kume (1), Hayato Go (1), Kazuhide Suyama (1), Mitsuaki Hosoya (1)

(1) Department of Pediatrics, Fukushima Medical University School of Medicine, Fukushima, Japan

(2) Department of Pediatrics, Sapporo Medical University School of Medicine, Hokkaido, Japan

*Correspondence: Yukihiko Kawasaki, 1 Hikarigaoka, Fukushima City, Fukushima 960-1295, Japan (1);

Minami 1-jo Nisi 17-chome, Chuo-ku, Sapporo City, Hokkaido 060-8556, Japan (2)

Tel.: +81-024-547-1295; Fax: +81-024-548-6578; Email: kyuki@fmu.ac.jp

**Running head:** HMGB1 involvement in murine HUS pathogenesis

**Abstract**

Typical hemolytic uremic syndrome is caused by the Shiga toxin (Stx2) and lipopolysaccharide (LPS) of *Escherichia coli* and leads to acute kidney injury. The role of innate immunity in this pathogenesis is unclear. We analyzed the role of high-mobility group box 1 (HMGB1) at the onset of disease in a murine model.

C57BL/6 mice were intraperitoneally administered with saline (Group A); anti-HMGB1 monoclonal antibody (Group B); Stx2 and LPS, to elicit severe disease (Group C); or Stx2, LPS, and anti-HMGB1 antibody (Group D).

While all Group C mice died by day 5 of the experiment, all Group D mice survived. Anemia and thrombocytopenia were pronounced, and plasma creatinine levels were significantly elevated in Group C only at 72 h. While at 72 h after toxin administration the glomerulus tissue in Group C showed pathology similar to that of humans, mesangial cell proliferation was seen in Group D. Plasma HMGB1 levels in Group C peaked 3 h after administration and were higher than those in other groups. Expression of the receptor of advanced glycation end-products and nuclear factor κB, involved in HMGB1 signaling, was significantly elevated in Group C but not in Group D. Administration of anti-HMGB1 antibody in a murine model of severe disease inhibited plasma HMGB1 and promoted amelioration of tissue damage. HMGB1 was found to be involved in the disease pathology; therefore, controlling HMGB1 activity might inhibit disease progression.

**Keywords**: acute kidney injury, hemolytic uremic syndrome, HMGB1, cell death, cytokines

## Introduction

Typical hemolytic uremic syndrome (tHUS), defined as a triad of microangiopathic hemolytic anemia, thrombocytopenia, and acute kidney injury, is a typical renal disease with endothelial cell dysfunction. Under electron microscopy (EM) examination, endothelial swelling and detachment from the basement membrane are observed in this disease [15, 16, 18, 26]. In most infant cases, the disease is caused by an infection with Shiga toxin 2 (Stx2) and lipopolysaccharide (LPS) produced by *Escherichia coli*, and is the most common cause of acute renal failure in children [16, 18]. Large-scale outbreaks of tHUS have recently been reported in Japan and 15 countries in Europe [16]. The mortality of tHUS has been reported to be between 3 and 5%, and death from tHUS is nearly always associated with severe extrarenal disease, including central nervous system involvement. Approximately two-thirds of children with tHUS require dialysis therapy; approximately one-third show milder renal involvement without the need for dialysis [15, 16, 18, 26]. It is necessary to follow-up on tHUS patients over their entire lifetime, since the disease is associated with a variety of sequelae, such as chronic kidney disease [30], neurological sequelae [7, 27], and endocrine dysfunction [31, 31a]. Because a standard treatment for tHUS has not yet been established, further clarification of the pathology and efficient drugs are necessary.

Elevated plasma levels of tumor necrosis factor-alpha (TNF-α) and interleukin (IL) 6 in patients with tHUS are consistently reported. Indeed, circulating levels of TNF-α and IL-6 correlate with tHUS severity and the occurrence of extrarenal complications [24, 28]. It is hence thought that such circulating factors are associated with tHUS development. The inhibition of inflammatory cytokines, therefore, may present a strategy against tHUS.

Pattern-recognition receptors (PRRs), such as Toll-like receptors, nucleotide-binding oligomerization domain-containing protein 2, and the receptor of advanced glycation end-products (RAGE), are innate immune system receptors. They recognize pathogen-associated molecular patterns (PAMPs), which are structural components of a variety of microbes, and activate the innate

immune system. In addition, PRRs appear to recognize damage-associated molecular patterns (DAMPs), which are released by dead or dying cells, particularly by cells that face unscheduled death. Activation of the innate immune system by both PAMPs and DAMPs stimulates the production of pro-inflammatory cytokines, e.g., TNF-α and IL-6, and affects the migration of immune cells, including neutrophils, macrophage, and monocytes, and the maturation of dendric cells [5, 11, 19].

High mobility group box-1 (HMGB1) was originally identified as a ubiquitous DNA-binding protein [10] and is now also recognized as a DAMP [14]. HMGB1 has been proposed to be a crucial mediator in the pathogenesis of many diseases, such as sepsis [38], autoimmunity [6], and acute lung inflammation [1]. The molecule can be released passively by necrotic cells, and/or actively secreted by macrophages or monocytes into the extracellular milieu [21]. Extracellular HMGB1 can elicit the production of proinflammatory cytokines that induce inflammatory responses through several immune receptors, including TLR4 [41] and RAGE [12, 37].

Since tHUS is a microangiopathy caused by an *E. coli* infection, PAMPs and DAMPs are thought to be involved in its development. However, only a few reports on the association between PAMPs and DAMPs, and the development of tHUS have been published. Here, we investigated the role of HMGB1 in tHUS and explored whether anti-HMGB1 monoclonal antibody (mAb) can inhibit tHUS development by inhibiting HMGB1 activity in a mouse model of tHUS.

## Materials and methods

### Animal Ethics

The current study was approved by the Control of the Animal Research Committee in accordance with the Guidelines on Animal Experiments in Fukushima Medical University (FMU), and the Rules for the Protection and Care of Animals (approval number 29075). All experiments were performed in compliance with the EU Directive 2010/63/EU for animal experiments (http://ec.europa.eu/environment/chemicals/lab_animals/legislation_en.htm).

### Experimental animals and establishment of the mouse tHUS model

Animal experiments involved 8-week-old male inbred C57BL/6 mice (20–25 g body weight, n = 100) (Japan SLC, Inc., Shizuoka, Japan). The animals had free access to water and a standard pellet diet and were monitored daily.

Stx2 was produced in the *E. coli* DH5α strain harboring the pLPSH3 plasmid, and purified using immunoaffinity chromatography [23, 32]. LPS (O55: B5) was purchased from Sigma-Aldrich (St. Louis, MO). As needed, the mice received intraperitoneal injections of Stx2 (225 ng/kg, 10.0 ml/kg) and LPS (300 μg/kg, 10.0 ml/kg) as previously described [17]. The time of Stx2 and LPS injection was defined as 0 h. Each mouse was checked for general symptoms of disease and weighed daily. Although the ethical endpoint was defined as the time when a mouse reached < 70% of its maximum weight, all mice in Group C died of natural causes before the ethical endpoint.

### Administration of anti-HMGB1 mAb to tHUS mouse

The anti-HMGB1 mAb (immunoglobulin G1 subclass; Antibodies-Online, Atlanta, GA) was administered by intraperitoneal injection (0.5 mg/kg, 10.0 ml/kg). The dose of anti-HMGB1 mAb (0.5 mg/kg mouse) was considered sufficient, since a 7-d survival rate was unchanged upon administration of a larger dose (data not shown).

**Experimental protocol**

Mice were divided into four groups (n = 25 per group); those administered normal saline at 0 h (Group A, control) or anti-HMGB1 mAb at 0 h (Group B); tHUS model mice (Group C); and tHUS model mice administered with anti-HMGB1 mAb at 0 h (Group D). Each drug was administered as a peritoneal injection (10 ml/kg). Blood samples were collected from 5 mice in each group, under anesthesia with ketamine hydrochloride (80 mg/kg) and xylazine hydrochloride (10 mg/kg), at 0, 3, 6, 24, and 72 h after treatment administration. Mice were then sacrificed by cervical dislocation, and their kidneys were removed, cut into sections, and processed for LM, EM analysis and immunohistochemical microscopy (IHM).

**Survival rate analysis**

The survival rate for the tHUS model mice and those administered with anti-HMGB1 mAb was monitored daily until day 7 (n = 5). Then the rate of bodyweight decline was recorded daily for all mice.

**Histological examination of LM, EM and IHM**

*LM*

The renal tissue was fixed in buffered formalin and embedded in paraffin. Sections (2–3-μm thick) were individually stained with hematoxylin and eosin, PAS, and periodic acid-silver methenamine, then observed under a light microscope. Three independent evaluators semi-quantitatively graded the extracellular matrix accumulation in each quadrant at 20 glomeruli per kidney, on a scale from 0 to 3, as follows. Endothelial injury scores: (0) absence of mesangiolysis; (1) mesangial area exhibiting slight lucency (0–25% mesangial cells disrupted); (2) mesangial area exhibited moderate lucency (25–50%) with preservation of the underlying glomerular tuft architecture; and (3) mesangial area

exhibits marked lucency (50–100%) with degeneration and disruption of mesangial cells, usually in association with microaneurysm formation. Mesangial cell proliferation scores: 0, absence of mesangial cell proliferation; (1) slight increase in mesangial cell numbers; (2) moderate increase in mesangial cell numbers; and (3) a marked increase in mesangial cell numbers.

*EM*

A small portion of one pole of the kidney was minced into 1-mm cubes, fixed in 2.5% glutaraldehyde, then in 1% chrome-osmium solution, and embedded in Epon 812. Ultrathin sections were stained with uranyl acetate and lead citrate was examined and photographed using a Jem-1200EX electron microscope (Jeol, Ltd., Tokyo, Japan).

*IHM*

The immunoperoxidase staining for HMGB1 was evaluated as follows. Three observers semiquantitatively calculated the rate of HMGB1 negative cells per glomerular whole cells in each quadrant in 20 glomerular cells per kidney. Primary antibodies included rabbit anti-mouse HMGB1 polyclonal antibodies which were used for IHM (Abclonal Technology, Woburn, MA). The biotinylated secondary antibodies included an anti-rabbit ABC Staining System Kit (Santa Cruz Biotechnology Inc., Santa Cruz, CA) which was used for IHM with co-staining hematoxylin-eosin, according to manufacturers' instructions.

**Measurement of HMGB1, creatinine, and cytokine levels, and analysis of peripheral blood cells**

Mice were euthanized and whole blood was collected in hematology tubes containing tripotassium ethylenediaminetetraacetic acid for cell count analysis. Whole blood was left to coagulate at 25 °C for 10 min, after which the samples were centrifuged at 1500 × *g* at 4 °C for 10 min, and plasma was collected. Plasma HMGB1, creatinine, and plasma cytokine levels were then determined. HMGB1

and creatinine levels were measured using commercially available enzyme-linked immunosorbent assay kits (HMGB1: Shino-test, Kanagawa, Japan; creatinine: Wako Pure Chemical Industries, Ltd., Osaka, Japan). IL-6 and TNF-α levels were determined using a mouse cytokine/chemokine-magnetic bead panel (Millipore, Billerica, MA) and a Luminex 100 system (Millipore).

**Real-time polymerase chain reaction (PCR)**

Total RNA from the renal tissues was extracted using the mirVana miRNA isolation kit (Thermo Fisher Scientific, Waltham, MA) and subsequently used for mRNA level analysis. Total RNA concentration was determined using the Qubit 3 fluorometer (Thermo Fisher Scientific). RNA was reverse-transcribed to complementary DNA (cDNA) using the high-capacity cDNA reverse transcription kit (Thermo Fisher Scientific) and the iCycler (Bio-Rad Laboratories, Inc. Hercules, CA), according to the manufacturers' instructions. The cDNA was used as a template for PCR using the QuantStudio 6 Flex real-time PCR system (Thermo Fisher Scientific). To analyze gene expression, real-time PCR was performed using the TaqMan gene expression systems (Thermo Fisher Scientific), according to the manufacturer's protocol. The following TaqMan primers were used for analysis of gene expression: *Gapdh*, Mm99999915_g1; *Rage*, Mm01134790_g1; and *Nfkb* (p65), Mm00501346_m1. Data were normalized to *Gapdh* expression using the comparative cycle threshold (ΔΔCt) method.

**Statistics**

Values are expressed as the mean ± SD. Data were analyzed by the Steel-Dwass test, Mann-Whitney *U* test, and log-rank test (Kaplan-Meier). Statistical analysis was performed using Ekuseru-Toukei 2012 Excel add-in statistical analysis software (Social Survey Research Information Co. Ltd., Tokyo, Japan). A $P$-value of $< 0.05$ was considered statistically significant.

## Results

### Anti-HMGB1 mAb significantly improved the survival and body weight decline in the mouse tHUS model

For the mouse model of tHUS, the survival rate and body weight loss ratios in Groups C and D are shown in Figures 1a and 1b, respectively. All Group C mice died by day 5 of the experiment, whereas all Group D animals survived ($P < 0.01$). While the body weight loss in Group D was small, that in Group C was prominent 4 d after disease onset. The body weight loss ratio in Group C 5 d after disease onset was lower than that in Group D (–18.2 ± 2.5% vs. –10.2 ± 4.4%, $P < 0.05$).

### Anti-HMGB1 mAb improved the tHUS triad: intergroup comparison of the peripheral blood cell counts and plasma creatinine levels

The erythrocyte count in Group C at 72 h was significantly lower than that in all other groups (776.4 ± 75.6 × $10^4$/μl, $P < 0.05$; Fig. 2a). Fragmented erythrocytes were observed in Group C mice 72 h after the administration of Stx2 and LPS (Fig. 2b).

The platelet count in Group C at 72 h was lower than that in all other groups (15.3 ± 3.9 × $10^4$/μl, $P < 0.05$; Fig. 2c). Although the platelet count in Group D indicated thrombocytopenia at 24 h, it improved at 72 h. No significant difference in platelet counts was apparent among Groups A, B, and D after 72 h.

The plasma creatinine levels in Group C at 72 h were higher than those in all other groups (0.7 ± 0.2 mg/dl, $P < 0.05$; Fig. 2d). Although the plasma creatinine levels in Group D tended to be elevated after 6 h, there were no significant differences between that group, and Groups A and B.

### Anti-HMGB1 mAb significantly reduced kidney injury after the administration of Stx2 and LPS

*Light microscopy (LM) findings*

Endothelial injury in Groups C and D developed gradually, 3 h after the administration of tested compounds (Fig. 3a). Group C endothelial injury scores at the tested time-points were all higher than those in other groups ($P < 0.05$). Compared to the endothelial injury scores in Group C, those in Group D were milder and peaked at 24 h.

Although there were no significant differences in the mesangial cell proliferation scores in Group C during disease development, those in Group D increased gradually after administration of Stx2, LPS, and HMGB1 mAb (Fig. 3b).

No mesangiolysis, cystic dilation, mesangial cell proliferation, or increase in the mesangial matrices were apparent in Groups A and B (Fig. 4a and 4b, respectively). Severe mesangiolysis and cystic dilation of the glomerular tuft were observed, but no mesangial cell proliferation or increase in mesangial matrices were noted, in Group C (Fig. 4c). Slight cystic dilatation of the glomerular tuft and mesangial cell proliferation were seen in Group D (Fig. 4d).

*EM findings*

The EM findings at 72 h, for Groups C and D, are shown in Figure 4. In Group C, degeneration of endothelial cells and cystic dilatation of the glomerular tuft, presence of a fibrin-like substance, and abnormal hemocoagulation were noted (Fig. 4e). In Group D, the structure of the glomerular tuft was maintained, and the endothelial cells formed immature capillary-like lumina (Fig. 4f).

IHM findings

The IHM findings and glomerular HMGB1 negative staining rates for all groups are shown in Figure 5. The non-injured cells were stained with brown in nuclear HMGB1. An increased tendency was observed during immunostaining of the negative cells in Group C (Fig. 5a) and D (Fig. 5d), and at 6 h, those in Group C were more numerous than those in Group D. Moreover, the negative rates for HMGB1 staining of Group C were higher than those in other groups at 6 h and 72 h ($P < 0.01$; Fig.

5e).

**Involvement of HMGB1 in disease development of the mouse tHUS model: anti-HMGB1 mAb inhibited the release of IL-6 and TNF-α after Stx2 and LPS administration**

After 3 h, plasma HMGB1 levels in Group C were higher than those in the other groups (3 h: 248.4 ± 30.6 ng/ml, $P < 0.05$; Fig. 6a). Plasma HMGB1 levels in Groups B and D increased slightly, but not significantly, after 24 h.

Plasma TNF-α levels in Group C peaked after 6 h and were higher than those in the other groups (64.9 ± 13.8 pg/ml, $P < 0.05$; Fig 6b). The levels in Group D peaked after 3 h, were lower than those in Group C, and were suppressed from 6 h onwards.

After 3 and 6 h, the plasma IL-6 levels in Group C were higher than those in other groups (3 h: 6117.8 ± 2304.6 pg/ml, $P < 0.05$; 6 h: 1414.5 ± 516.0 pg/ml, $P < 0.05$; Fig. 6c).

**Anti-HMGB1 mAb attenuated RAGE and nuclear factor (NF) κB expression in the kidney after Stx2 and LPS administration**

Since RAGE and NF-κB are involved in HMGB1 signaling [3], expression of the encoding genes was compared across all Groups at 0, 6, and 72 h. Kidney expression of *Rage* and *Nfkb* genes in all groups are shown in Figures 7a and 7b, respectively. The normalized expression of both genes in Group C was higher than that in other groups (*Rage*: 6 h: 3.6 ± 0.7, $P < 0.05$, 72 h: 2.3 ± 0.5, $P < 0.05$; *Nfkb*: 6 h: 4.2 ± 1.3, $P < 0.05$, 72 h: 3.0 ± 0.5, $P < 0.05$). In contrast, no such increase was apparent in Group D at 6 and 72 h.

**Discussion**

In the current study, we investigated the role of HMGB1 in the development of tHUS and the possibility of administering anti-HMGB1 mAb as a possible tHUS treatment, in the mouse model.

We observed that all Group C mice, which had received Stx2 and LPS, died by day 5 following administration, whereas all Group D mice, were additionally administered with anti-HMGB1 mAb, and survived the observation period. The tHUS triad was not apparent in Group D. Further, although endothelial cell injury was noted in Group C animals, only mild endothelial cell injury was apparent in the Group D animals. Mesangial proliferation was observed in Group D animals, reflecting improvement in tissue injury because of HMGB1 inhibition with anti-HMGB1 mAb. HMGB1 staining negative rates were observed in Group C and D, which indicated HMGB1 was released extracellularly via tHUS development. While HMGB1 staining negative rates increased in the Group C animals, only mild increases in rates were apparent in Group D animals. High plasma HMGB1 levels were only observed in Group C, which indicated the release of HMGB1 extracellularly and the association of HMGB1 with tHUS development. Accordingly, the increase of *Rage* and *Nfkb* expression involved in HMGB1 signaling was significantly inhibited by anti-HMGB1 mAb in Group D, and IL-6 and TNF-α levels were suppressed by a positive-feedback inhibition.

Various animal models have been used to investigate the pathology of tHUS. Although the baboon model of tHUS, reported by Taylor, exhibited a pathology similar to human tHUS, its full pathophysiology has not been completely investigated [34]. Since large animal models are usually expensive and impractical, small animal models were developed subsequently. In 2004, Ikeda et al. reported that LPS and Stx2 could be used to establish a tHUS mouse model [13]. In 2006, Keepers et al. reported that C57BL/6 mice induced by LPS and Stx2 could be used to model the triad of tHUS in humans [17]. Although this mouse model does not reflect the precise HUS found in humans as described below in the limitations, this mouse model has been useful for the identification of therapeutic targets and the development of new treatments for tHUS. Indeed, we had previously reported the involvement of vascular endothelial growth factor in the recovery process after renal injury and the efficacy of recombinant human soluble thrombomodulin in tHUS [23, 32].

HMGB1, a DAMP, is an evolutionarily conserved protein that is abundant in the nuclei of

almost all eukaryotic cells. Originally, this protein was thought to mainly function as a nonhistone chromatin-binding protein, stabilizing the chromatin structure and modulating gene transcription [29]. HMGB1 was also reported to be passively released extracellularly via processes such as cell death, and upon cell stimulation by PRR ligands, such as LPS [5]. Extracellular HMGB1 molecules are considered to be recognized by PRRs, such as RAGE, thereby inducing inflammatory cytokines, such as TNF-α and IL-6, mainly by activating the NF-κB pathway [3]. Furthermore, RAGE is the primary binding receptor for HMGB1, and the interaction between RAGE and HMGB1 induces an inflammatory response via NF-κB activation [14]. HMGB1-induced signaling can result in the expression of RAGE via a positive feedback loop [36], activating the NF-κB pathway, and facilitating the immune response. Since HMGB1 signaling promotes inflammation, HMGB1 is implicated in various disease states, such as sepsis [39], ischemia-reperfusion [35], arthritis [2], meningitis [33], neurodegeneration [25], aging [9], and cancer [20]. HMGB1 antagonists have been reported to improve the state of such diseases as sepsis and pneumonia, induced by influenza A virus (H1N1) in animal models [22, 38]. Consequently, effective regulation of HMGB1 signaling has been receiving a lot of attention recently. Although it is thought that both PAMPs and DAMPs are associated with tHUS development because tHUS is a form of microangiopathy caused by *E. coli* infection, the association between the development of tHUS and HMGB1 has not been reported to date.

According to the manufacturer (Antibodies-Online), anti-HMGB1 mAb used in the current study was monoclonal and recognized the C-terminal sequence of HMGB1 (box B) located near the RAGE-binding domain. Hence, in the current study, we speculated that ① the extracellular release of HMGB1 was triggered by *E. coli* infection and tHUS microangiopathy stimulated RAGE; ② cytokines including TNF-α and IL-6 were released by activating the NF-κB pathway induced by HMGB1–RAGE signaling; ③ furthermore, the positive feedback loop was induced with HMGB1 and released by tHUS development. We also speculated that the extracellular release of HMGB1

triggered by the *E. coli* infection and tHUS microangiopathy were inhibited by anti-HMGB1 mAb, and the ensuing development of tHUS and kidney injury was moderated due to the inhibition of HMGB1–RAGE signaling and the positive-feedback loop between HMGB1 and the proinflammatory cytokines, including TNF-α and IL-6.

One limitation of the current study was that the features of the mouse model of tHUS did not fully recapitulate tHUS in humans, since the mouse glomerular endothelium lacks the Gb3 receptor [17]. To further evaluate the efficacy of anti-HMGB1 mAb for tHUS treatment, it would be necessary to investigate it in the baboon model of tHUS, where Gb3 receptor is present. Furthermore, we focused on the association between HMGB1 and tHUS development; however, to evaluate a possible new therapy for tHUS, further studies of the dose and frequency of anti-HMGB1 mAb administration, as a post-treatment regimen in tHUS models, would be necessary. Finally, we did not use HMGB1 knock-out mice in the current study because it has been reported that all newborn *HMGB1*$^{-/-}$ mice die within a few days [8], and the HMGB1 conditional knock-out mice are more sensitive to endotoxin shock induced by LPS compared with the control mice [40]. Although it may be effective to use HMGB1 hetero mice, which is a speculative model with partial inhibition of HMGB1, little is known about the role of HMGB1 in inflammation. Therefore, further research will be necessary in the future.

In conclusion, we revealed the involvement of HMGB1 in the development of tHUS. Administration of anti-HMGB1 antibody in a murine model of severe tHUS inhibited plasma HMGB1 and cytokine release, and ameliorated tissue damage. These observations suggested that controlling HMGB1 signaling may inhibit the progress of tHUS.

**Acknowledgements**

We are grateful to Mieko Tanji and Sakurako Norito for their excellent technical assistance.

**Disclosures:**

**Conflicts of interest:** None declared.

**References**


1. **Abraham E, Arcaroli J, Carmody A, Wang H, Tracey KJ.** HMG-1 as a mediator of acute lung inflammation. J Immunol 165: 2950–2954, 2000. https://doi.org/10.4049/jimmunol.165.6.2950. PubMed
2. **Andersson U, Tracey KJ.** HMGB1 as a mediator of necrosis-induced inflammation and a therapeutic target in arthritis. Rheum Dis Clin North Am 30: 627–637, 2004. https://doi.org/10.1016/j.rdc.2004.04.007. PubMed
3. **Andersson U, Tracey KJ.** HMGB1 is a therapeutic target for sterile inflammation and infection. Annu Rev Immunol 29: 139–162, 2011. https://doi.org/10.1146/annurev-immunol-030409-101323. PubMed
5. **Bianchi ME, Crippa MP, Manfredi AA, Mezzapelle R, Rovere Querini P, Venereau E.** High-mobility group box 1 protein orchestrates responses to tissue damage via inflammation, innate and adaptive immunity, and tissue repair. Immunol Rev 280: 74–82, 2017. https://doi.org/10.1111/imr.12601. PubMed
6. **Bianchi ME, Manfredi AA.** High-mobility group box 1 (HMGB1) protein at the crossroads between innate and adaptive immunity. Immunol Rev 220: 35–46, 2007. https://doi.org/10.1111/j.1600-065X.2007.00574.x. PubMed
7. **Brasher C, Siegler RL.** The hemolytic-uremic syndrome. West J Med 134: 193–197, 1981. PubMed
8. **Calogero S, Grassi F, Aguzzi A, Voigtländer T, Ferrier P, Ferrari S, Bianchi ME.** The lack of chromosomal protein Hmg1 does not disrupt cell growth but causes lethal hypoglycaemia in newborn mice. Nat Genet 22: 276–280, 1999. https://doi.org/10.1038/10338. PubMed
9. **Enokido Y, Yoshitake A, Ito H, Okazawa H.** Age-dependent change of HMGB1 and DNA double-strand break accumulation in mouse brain. Biochem Biophys Res Commun 376: 128–133, 2008. https://doi.org/10.1016/j.bbrc.2008.08.108. PubMed

10. **Goodwin GH, Johns EW.** Isolation and characterisation of two calf-thymus chromatin non-histone proteins with high contents of acidic and basic amino acids. Eur J Biochem 40: 215–219, 1973. https://doi.org/10.1111/j.1432-1033.1973.tb03188.x. PubMed

11. **Heilmann RM, Allenspach K.** Pattern-recognition receptors: signaling pathways and dysregulation in canine chronic enteropathies-brief review. J Vet Diagn Invest 29: 781–787, 2017. https://doi.org/10.1177/1040638717728545. PubMed

12. **Hori O, Brett J, Slattery T, Cao R, Zhang J, Chen JX, Nagashima M, Lundh ER, Vijay S, Nitecki D, Morser J, Stern D, Schmidt AM.** The receptor for advanced glycation end products (RAGE) is a cellular binding site for amphoterin. Mediation of neurite outgrowth and co-expression of rage and amphoterin in the developing nervous system. J Biol Chem 270: 25752–25761, 1995. https://doi.org/10.1074/jbc.270.43.25752. PubMed

13. **Ikeda M, Ito S, Honda M.** Hemolytic uremic syndrome induced by lipopolysaccharide and Shiga-like toxin. Pediatr Nephrol 19: 485–489, 2004. https://doi.org/10.1007/s00467-003-1395-7. PubMed

14. **Kang R, Chen R, Zhang Q, Hou W, Wu S, Cao L, Huang J, Yu Y, Fan XG, Yan Z, Sun X, Wang H, Wang Q, Tsung A, Billiar TR, Zeh HJ III, Lotze MT, Tang D.** HMGB1 in health and disease. Mol Aspects Med 40: 1–116, 2014. https://doi.org/10.1016/j.mam.2014.05.001. PubMed

15. **Karmali MA, Petric M, Lim C, Fleming PC, Arbus GS, Lior H.** The association between idiopathic hemolytic uremic syndrome and infection by verotoxin-producing Escherichia coli. J Infect Dis 151: 775–782, 1985. https://doi.org/10.1093/infdis/151.5.775. PubMed

16. **Karpman D, Sartz L, Johnson S.** Pathophysiology of typical hemolytic uremic syndrome. Semin Thromb Hemost 36: 575–585, 2010. https://doi.org/10.1055/s-0030-1262879. PubMed

17. **Keepers TR, Psotka MA, Gross LK, Obrig TG.** A murine model of HUS: Shiga toxin with lipopolysaccharide mimics the renal damage and physiologic response of human disease. J Am Soc Nephrol 17: 3404–3414, 2006. https://doi.org/10.1681/ASN.2006050419. PubMed

18. **Keir L, Coward RJ.** Advances in our understanding of the pathogenesis of glomerular thrombotic microangiopathy. Pediatr Nephrol 26: 523–533, 2011. https://doi.org/10.1007/s00467-010-1637-4. PubMed

19. **Krysko DV, Garg AD, Kaczmarek A, Krysko O, Agostinis P, Vandenabeele P.** Immunogenic cell death and DAMPs in cancer therapy. Nat Rev Cancer 12: 860–875, 2012. https://doi.org/10.1038/nrc3380. PubMed

20. **Lotze MT, DeMarco RA.** Dealing with death: HMGB1 as a novel target for cancer therapy. Curr Opin Investig Drugs 4: 1405–1409, 2003. PubMed

21. **Magna M, Pisetsky DS.** The role of HMGB1 in the pathogenesis of inflammatory and autoimmune diseases. Mol Med 20: 138–146, 2014. https://doi.org/10.2119/molmed.2013.00164. PubMed

22. **Nosaka N, Yashiro M, Yamada M, Fujii Y, Tsukahara H, Liu K, Nishibori M, Matsukawa A, Morishima T.** Anti-high mobility group box-1 monoclonal antibody treatment provides protection against influenza A virus (H1N1)-induced pneumonia in mice. Crit Care 19: 249, 2015. https://doi.org/10.1186/s13054-015-0983-9. PubMed

23. **Ohara S, Kawasaki Y, Abe Y, Watanabe M, Ono A, Suyama K, Hashimoto K, Honda T, Suzuki J, Hosoya M.** Role of vascular endothelial growth factor and angiopoietin 1 in renal injury in hemolytic uremic syndrome. Am J Nephrol 36: 516–523, 2012. https://doi.org/10.1159/000345142. PubMed

24. **Proulx F, Litalien C, Turgeon JP, Mariscalco MM, Seidman E.** Circulating levels of transforming growth factor-beta1 and lymphokines among children with hemolytic uremic syndrome. Am J Kidney Dis 35: 29–34, 2000. https://doi.org/10.1016/S0272-6386(00)70297-6. PubMed

25. **Qi ML, Tagawa K, Enokido Y, Yoshimura N, Wada Y, Watase K, Ishiura S, Kanazawa I, Botas J, Saitoe M, Wanker EE, Okazawa H.** Proteome analysis of soluble nuclear proteins

reveals that HMGB1/2 suppress genotoxic stress in polyglutamine diseases. Nat Cell Biol 9: 402–414, 2007. https://doi.org/10.1038/ncb1553. PubMed

26. **Scheiring J, Andreoli SP, Zimmerhackl LB.** Treatment and outcome of Shiga-toxin-associated hemolytic uremic syndrome (HUS). Pediatr Nephrol 23: 1749–1760, 2008. https://doi.org/10.1007/s00467-008-0935-6. PubMed

27. **Sheth KJ, Swick HM, Haworth N.** Neurological involvement in hemolytic-uremic syndrome. Ann Neurol 19: 90–93, 1986. https://doi.org/10.1002/ana.410190120. PubMed

28. **Shimizu M, Kuroda M, Inoue N, Konishi M, Igarashi N, Taneichi H, Kanegane H, Ito M, Saito S, Yachie A.** Extensive serum biomarker analysis in patients with enterohemorrhagic Escherichia coli O111-induced hemolytic-uremic syndrome. Cytokine 66: 1–6, 2014. https://doi.org/10.1016/j.cyto.2013.12.005. PubMed

29. **Sims GP, Rowe DC, Rietdijk ST, Herbst R, Coyle AJ.** HMGB1 and RAGE in inflammation and cancer. Annu Rev Immunol 28: 367–388, 2010. https://doi.org/10.1146/annurev.immunol.021908.132603. PubMed

30. **Spinale JM, Ruebner RL, Copelovitch L, Kaplan BS.** Long-term outcomes of Shiga toxin hemolytic uremic syndrome. Pediatr Nephrol 28: 2097–2105, 2013. https://doi.org/10.1007/s00467-012-2383-6. PubMed

31. **Suri RS, Mahon JL, Clark WF, Moist LM, Salvadori M, Garg AX.** Relationship between Escherichia coli O157:H7 and diabetes mellitus. Kidney Int Suppl 75: S44–S46, 2009. https://doi.org/10.1038/ki.2008.619. PubMed

31a. **Suri RS, Clark WF, Barrowman N, Mahon JL, Thiessen-Philbrook HR, Rosas-Arellano MP, Zarnke K, Garland JS, Garg AX.** Diabetes during diarrhea-associated hemolytic uremic syndrome: a systematic review and meta-analysis. Diabetes Care 28: 2556–2562, 2005. https://doi.org/10.2337/diacare.28.10.2556. 16186301

32. **Suyama K, Kawasaki Y, Miyazaki K, Kanno S, Ono A, Ohara S, Sato M, Hosoya M.** The

efficacy of recombinant human soluble thrombomodulin for the treatment of shiga toxin-associated hemolytic uremic syndrome model mice. Nephrol Dial Transplant 30: 969–977, 2015. https://doi.org/10.1093/ndt/gfv004. PubMed

33. **Tang D, Kang R, Cao L, Zhang G, Yu Y, Xiao W, Wang H, Xiao X.** A pilot study to detect high mobility group box 1 and heat shock protein 72 in cerebrospinal fluid of pediatric patients with meningitis. Crit Care Med 36: 291–295, 2008. https://doi.org/10.1097/01.CCM.0000295316.86942.CE. PubMed

34. **Taylor FB Jr, Tesh VL, DeBault L, Li A, Chang AC, Kosanke SD, Pysher TJ, Siegler RL.** Characterization of the baboon responses to Shiga-like toxin: descriptive study of a new primate model of toxic responses to Stx-1. Am J Pathol 154: 1285–1299, 1999. https://doi.org/10.1016/S0002-9440(10)65380-1. PubMed

35. **Tsung A, Sahai R, Tanaka H, Nakao A, Fink MP, Lotze MT, Yang H, Li J, Tracey KJ, Geller DA, Billiar TR.** The nuclear factor HMGB1 mediates hepatic injury after murine liver ischemia-reperfusion. J Exp Med 201: 1135–1143, 2005. https://doi.org/10.1084/jem.20042614. PubMed

36. **van Beijnum JR, Buurman WA, Griffioen AW.** Convergence and amplification of toll-like receptor (TLR) and receptor for advanced glycation end products (RAGE) signaling pathways via high mobility group B1 (HMGB1). Angiogenesis 11: 91–99, 2008. https://doi.org/10.1007/s10456-008-9093-5. PubMed

37. **van Zoelen MA, van der Sluijs KF, Achouiti A, Florquin S, Braun-Pater JM, Yang H, Nawroth PP, Tracey KJ, Bierhaus A, van der Poll T.** Receptor for advanced glycation end products is detrimental during influenza A virus pneumonia. Virology 391: 265–273, 2009. https://doi.org/10.1016/j.virol.2009.05.032. PubMed

38. **Wang H, Bloom O, Zhang M, Vishnubhakat JM, Ombrellino M, Che J, Frazier A, Yang H, Ivanova S, Borovikova L, Manogue KR, Faist E, Abraham E, Andersson J, Andersson U, Molina PE, Abumrad NN, Sama A, Tracey KJ.** HMG-1 as a late mediator of endotoxin lethality

in mice. Science 285: 248–251, 1999. https://doi.org/10.1126/science.285.5425.248. PubMed

39. **Wang H, Yang H, Tracey KJ.** Extracellular role of HMGB1 in inflammation and sepsis. J Intern Med 255: 320–331, 2004. https://doi.org/10.1111/j.1365-2796.2003.01302.x. PubMed

40. **Yanai H, Matsuda A, An J, Koshiba R, Nishio J, Negishi H, Ikushima H, Onoe T, Ohdan H, Yoshida N, Taniguchi T.** Conditional ablation of HMGB1 in mice reveals its protective function against endotoxemia and bacterial infection. Proc Natl Acad Sci USA 110: 20699–20704, 2013. https://doi.org/10.1073/pnas.1320808110. PubMed

41. **Yang H, Hreggvidsdottir HS, Palmblad K, Wang H, Ochani M, Li J, Lu B, Chavan S, Rosas-Ballina M, Al-Abed Y, Akira S, Bierhaus A, Erlandsson-Harris H, Andersson U, Tracey KJ.** A critical cysteine is required for HMGB1 binding to Toll-like receptor 4 and activation of macrophage cytokine release. Proc Natl Acad Sci USA 107: 11942–11947, 2010. https://doi.org/10.1073/pnas.1003893107. PubMed

**Figure:**

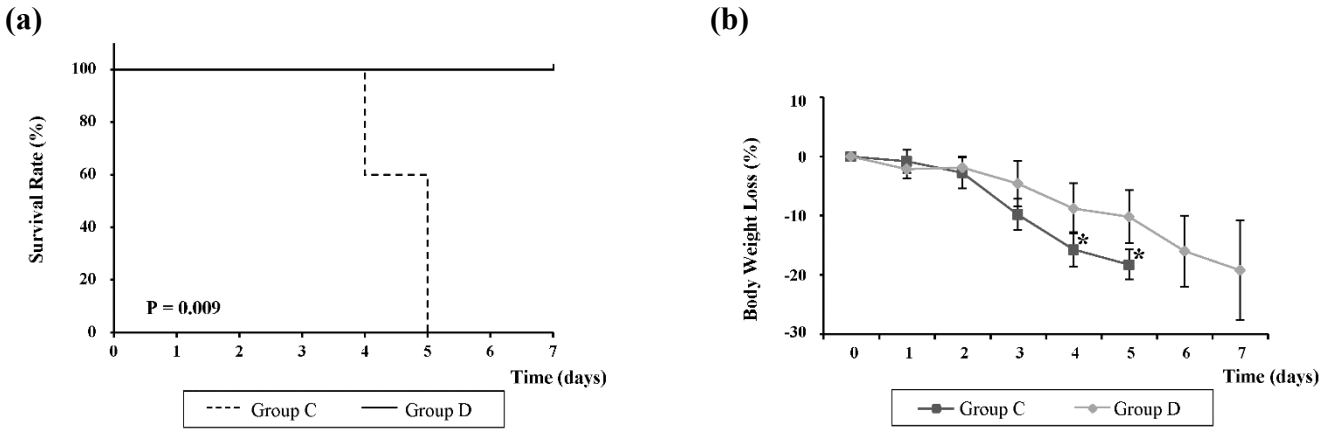


**Figure 1:** Comparison of the survival curves and the body weight loss between Group C and D animals. (a) Comparison of the survival curves using the log-rank test; $P = 0.009$ vs. Group C, n = 5 per group (b) Comparison of the body weight loss using the Mann-Whitney U test. Data are expressed as the mean ± SD; vs. Group D (*$P < 0.05$), n = 5 per group.

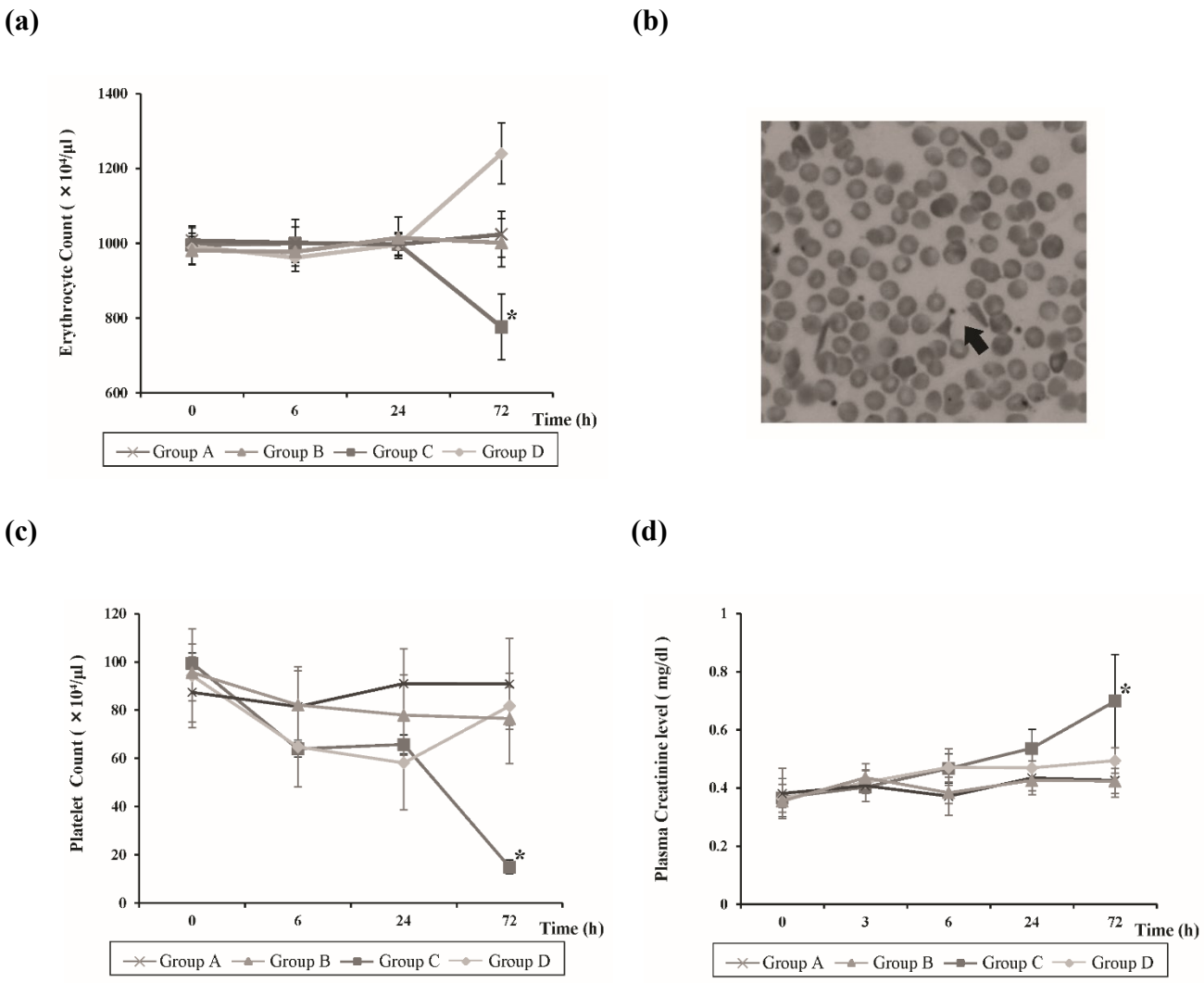


**Figure 2:** Intergroup comparison of the mean erythrocyte counts, mean platelet counts, and plasma creatinine levels. (a) Comparison of the erythrocyte count using the Steel-Dwass test. Data are expressed as the mean ± SD; **P* < 0.05 vs. each group, n = 5 per group per point. (b) Fragmented erythrocytes (arrow) were observed in the peripheral blood of Group C mice 72 h after Stx2 and LPS administration. (c) Comparison of the platelet count using the Steel-Dwass test. Data are expressed as the mean ± SD; **P* < 0.05 vs. each group, n = 5 per group per point. (d) Comparison of the plasma creatinine levels using the Steel-Dwass test. Data are expressed as the mean ± SD; **P* < 0.05 vs. each group, n = 5 per group per point.

**(a)** **(b)**

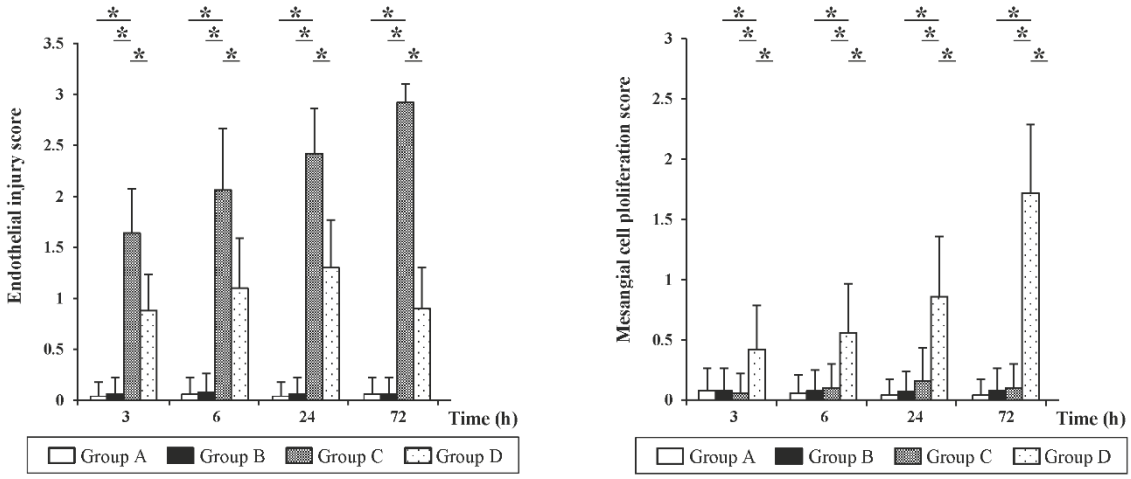


**Figure 3:** Intergroup comparison of the pathological finding scores. (a) Endothelial injury scores in mouse groups. Data are expressed as the mean ± SD; **P* < 0.05 vs. each group using the Steel-Dwass test, n =5 per group per point. (b) The mesangial cell proliferation scores in mouse groups. Data are expressed as the mean ± SD; **P* < 0.05 vs. each group using the Steel-Dwass test, n = 5 per group per point.

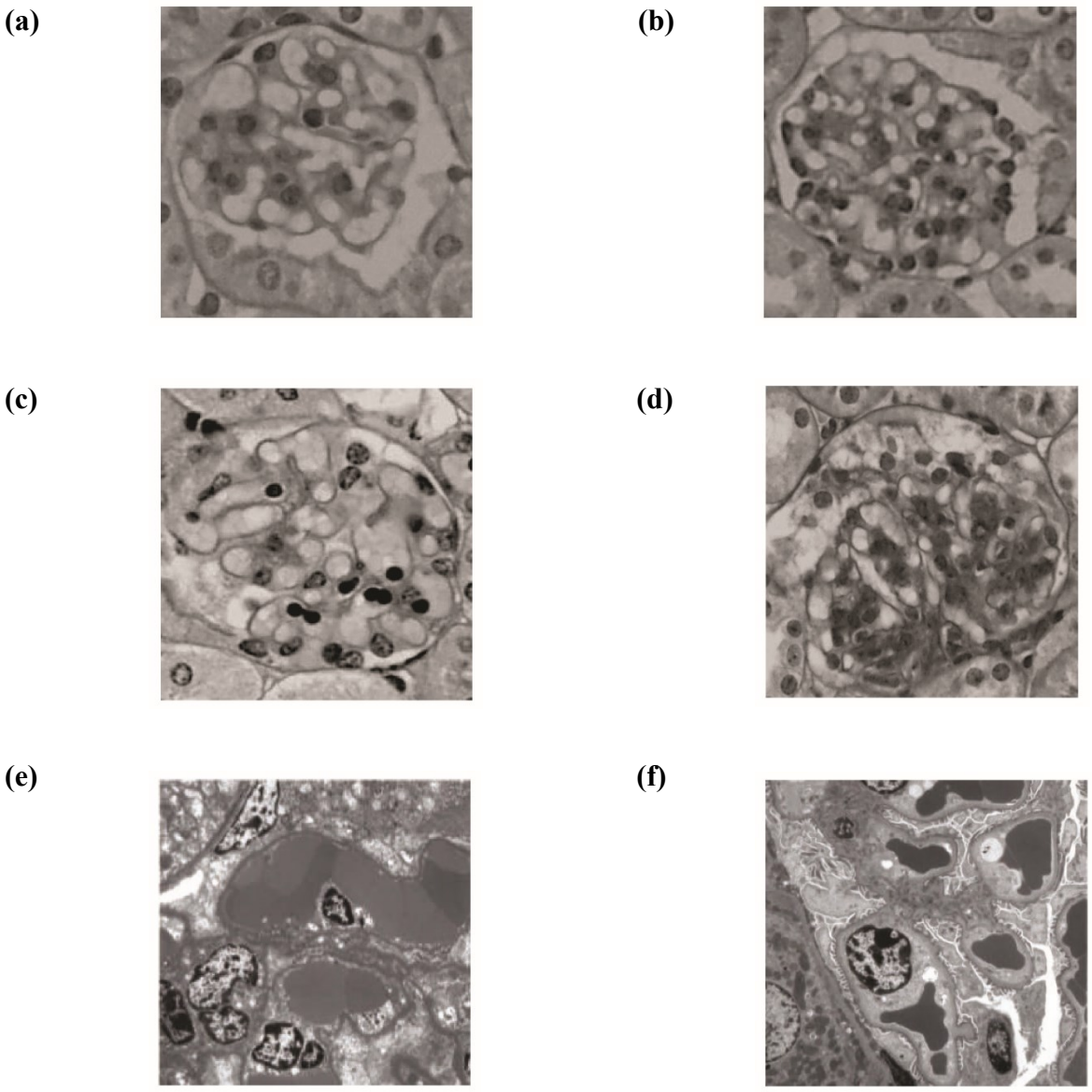


**Figure 4:** The effect of administration of various compounds on LM and EM findings in the murine model of tHUS. (a), (b) No mesangiolysis, cystic dilation, mesangial cell proliferation, or increase of the mesangial matrices were observed 72 h after the administration of normal saline or anti-HMGB1 mAb in Groups A (a) and B (b), respectively [LM finding, periodic acid-Schiff stain (PAS) ×400]. (c) 72 h after the administration of Stx2 and LPS in Group C, endothelial cell injury, severe mesangiolysis, and cystic dilation of the glomerular tuft were observed, but no mesangial cell proliferation or increase in the mesangial matrices were apparent (LM finding, PAS ×400). (d) Slight cystic dilatation of glomerular tuft and mesangial cell proliferation were observed 72 h after the administration of Stx2, LPS, and anti-HMGB1 mAB in Group D (LM finding, PAS ×400). The images are representative of

n = 5 biological replicates. (e) Severe mesangiolysis, degeneration of endothelial cells, cystic dilatation of the glomerular tuft, and abnormal coagulation were observed 72 h after the administration of Stx2 and LPS in Group C (EM finding, ×3000). (f) The structure of the glomerular tuft was maintained, and endothelial cells were observed forming immature capillary-like lumina 72 h after the administration of Stx2, LPS, and anti-HMGB1 mAb in Group D (EM finding, ×3000). The images are representative of n = 5 biological replicates.

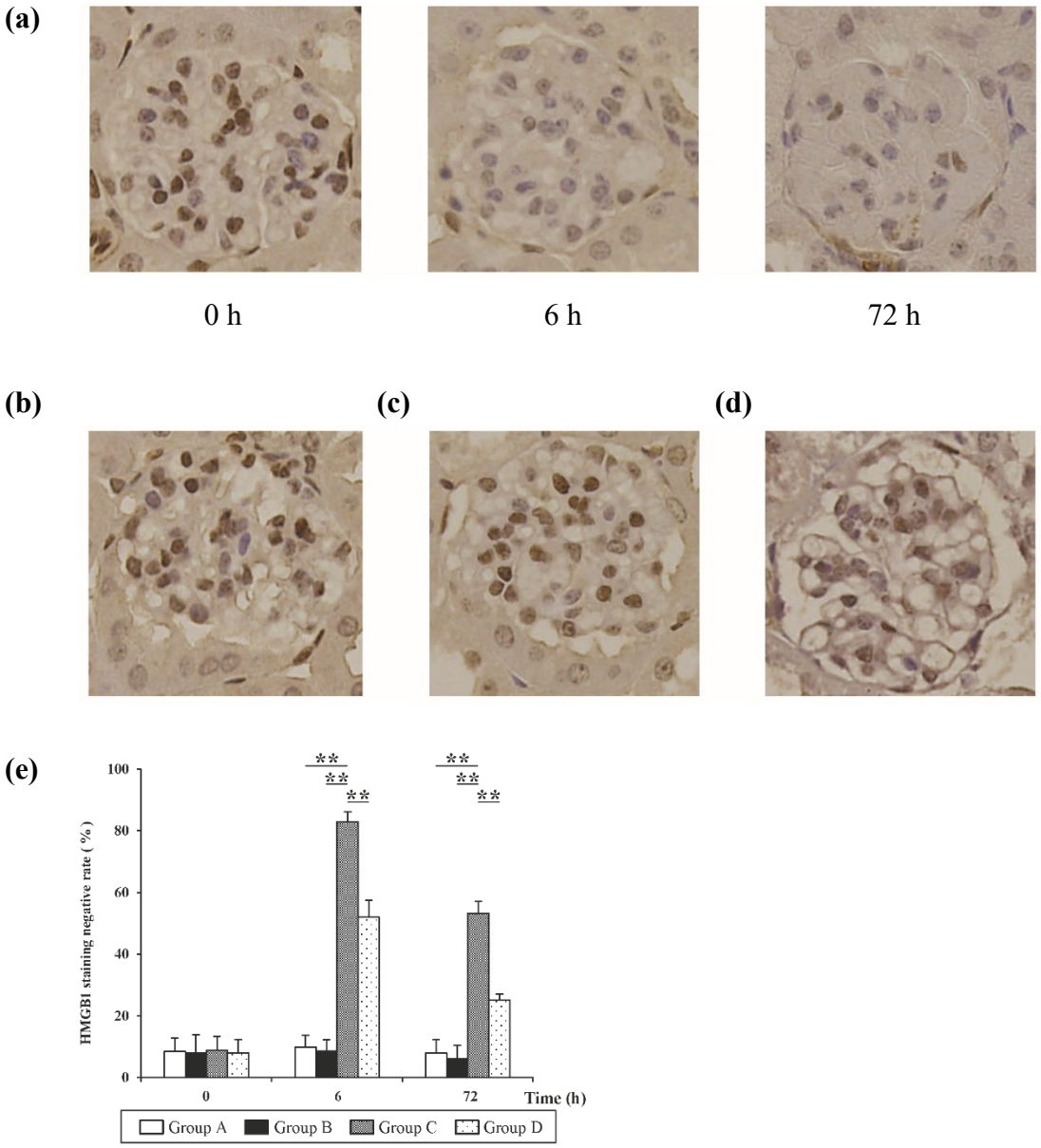


**Figure 5:** The effects of the administration of various compounds and the changes observed by immunostaining of HMGB1 over time in all groups (IHM finding, ×400). (a) HMGB1 negative cells tended to increase after the administration of Stx2 and LPS in Group C over time. (b), (c) HMGB1 negative cells were not increased 6 h after the administration of normal saline or anti-HMGB1 mAb in Groups A (b) and B (c), respectively. (d) HMGB1 negative cells were slightly increased 6 h after the administration of Stx2, LPS, and anti-HMGB1 mAB in Group D. (e) Intergroup comparison of the HMGB1 staining negative rates in mouse groups. Data are expressed as the mean ± SD; $^{**}P < 0.01$ vs. each group using the Steel-Dwass test, n=5 per group per point.

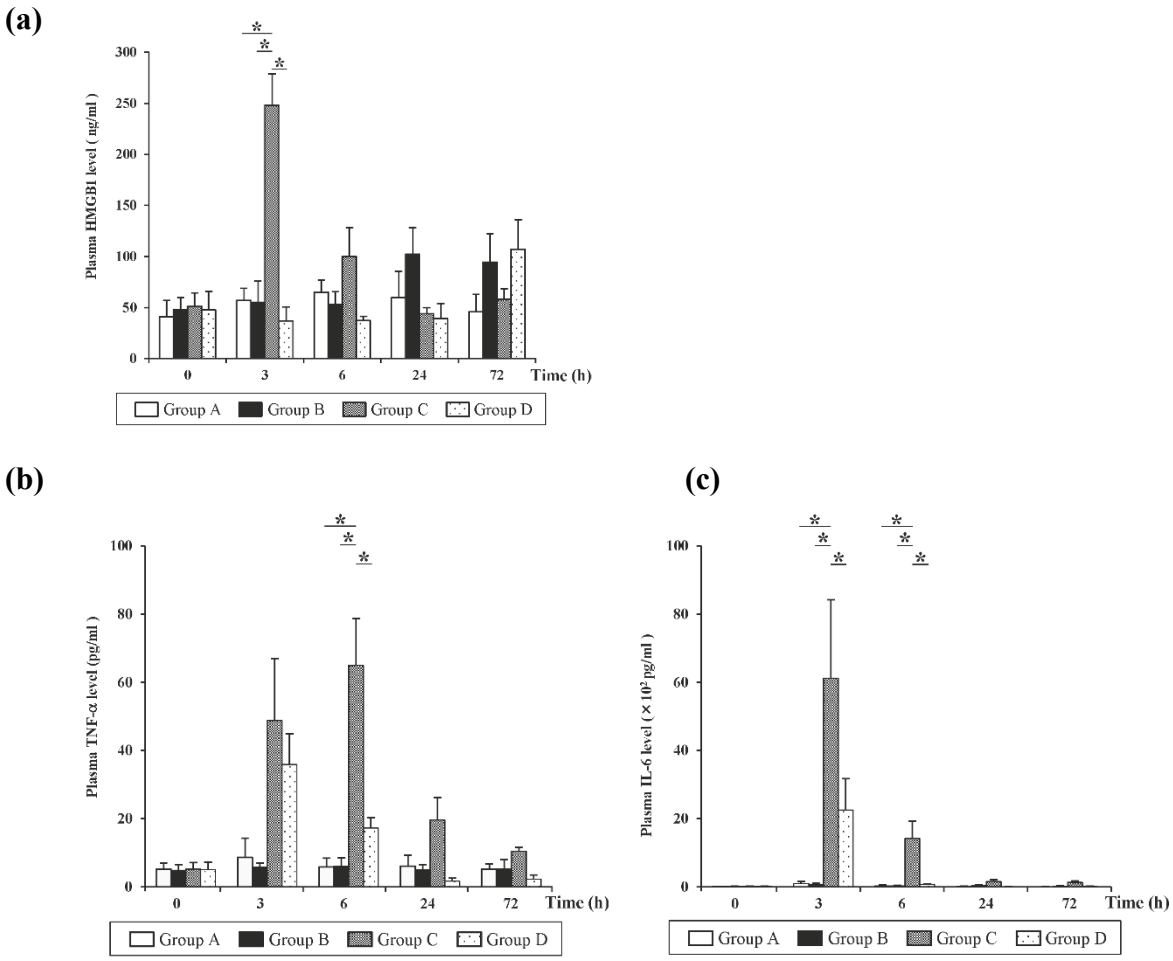


**Figure 6:** Intergroup comparison of the plasma HMGB1 levels and plasma cytokine levels. The data were compared using the Steel-Dwass test. (a) Comparison of the plasma HMGB1 levels. Data are expressed as the mean ± SD; **P* < 0.05 vs. each group, n = 5 per group per point. (b) Comparison of the plasma TNF-α levels; **P* < 0.05 vs. each group, n = 5 per group per point. (c) Comparison of the plasma IL-6 levels. Data are expressed as mean ± SD; **P* < 0.05 vs. each group, n = 5 per group per point.

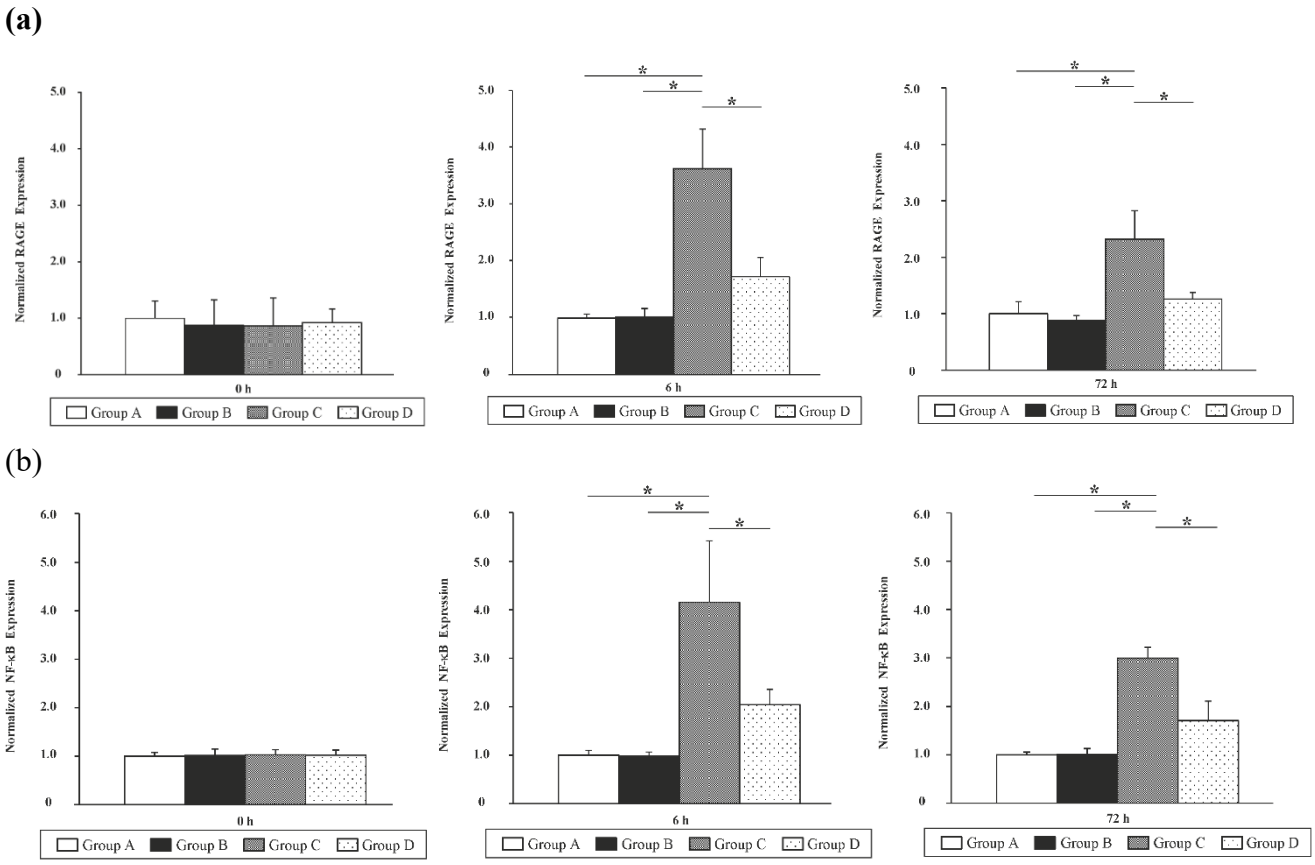


**Figure 7:** The renal expression of genes involved in HMGB1 signaling in different groups of animals. *Rage* (a) and *Nfkb* (p65) (b) mRNA levels in the kidney of animals from different groups were compared. The results were normalized to the expression of glyceralaldehyde-3-phosphate dehydrogenase (*Gapdh*) gene. The basal expression level in Group A mice was calibrated as 1.0. Data represent the mean ± SD; **P* < 0.05 vs. each group using the Steel-Dwass test, n = 5 per group per point.